The Photogrammetric Record 23(122): 128–147 (June 2008)

VIDEOGRAMMETRIC MONITORING OF AS-BUILT MEMBRANE ROOF STRUCTURES

SHIH-YUAN LIN* (syl@mssl.ucl.ac.uk)

JON P. MILLS (j.p.mills@ncl.ac.uk)

PETER D. GOSLING (p.d.gosling@ncl.ac.uk)
Newcastle University

Abstract

A monitoring system that uses applied geomatics techniques, including videogrammetry and terrestrial laser scanning, has been developed in order to investigate the dynamic behaviour of as-built membrane roof structures. To accommodate the problems involved in measuring such roof structures, examples of which include uniform surface texture and unreachable height, the system adopts a non-contact targeting methodology to substitute for traditional control techniques. In-house software was developed for processing the acquired video imagery in order to produce a sequential surface model of the membrane. This paper firstly reports on experiments conducted to demonstrate that the monitoring system was capable of measuring representative test structures with a precision of better than ±1 mm. To prove the feasibility and transferability of the system, videogrammetric monitoring campaigns were subsequently performed at a real-world test site where two different types of membrane structure were observed. The sequential 3D surface models that were generated allowed the displacement of the membrane surfaces to be investigated over a period, during which the range of the movement reached over 20 mm. The information acquired from the system is proving to be of great value to structural engineers involved in research and development of such membrane structures.

KEYWORDS: dynamic surface monitoring, membrane structure engineering, tensile architecture monitoring, videogrammetry

INTRODUCTION

THE TERM MEMBRANE STRUCTURE (or tensile architecture) refers to a building that is constructed from materials under tension. The term covers a broad category of structures, which includes fabric membranes, pre-stressed cable nets and cable beams in the form of trusses and girders. The essential elements of a membrane structure are (i) a highly flexible fabric held under tension in order to generate stiffness in the surface; (ii) one-dimensional flexible elements, such as ties or cables, to create ridges, valleys and edge boundaries; and (iii) rigid support members sustaining compression and bending (Lewis, 2003). Based on the different combinations of the above components, membrane structures are categorised into

**Now at Mullard Space Science Laboratory, University College London.*

three types: boundary-tensioned membranes, pneumatic structures, and pre-stressed cable nets and beams. Due to the advantage of fast construction speeds with extremely competitive unit costs, as well as the fact that such structures provide good durability with low maintenance, the number of membrane structures has increased significantly worldwide over the past decade and a half (Gosling, 2001).

This relatively new form of construction is most often adopted by engineers as the roof of a building. Different from conventional structural forms, membrane structures allow sufficient deflections to occur under imposed loads (including self-weight, wind and snow). When external loads are applied, the structure resists them by a combination of curvature and tension of the highly flexible fabric membrane, which is commonly made of PVC-coated polyester, Teflon-coated glass fibre (PTFE) or silicone-coated glass (Happold et al., 1987). Therefore, it is important at the design stage to calculate the strength and displacement which the fabric membrane requires in order to withstand the forces which are likely to be applied. Once the structure is built, collapse may occur if the real curvature and tension exceed the tolerances of the original design. In January 1999, for example, the new membrane roof over Montreal's Olympic Stadium failed, the cause of failure identified as a design fault, not an accident (Parker, 1999a, b). To avoid such failures in future, further research into realising the behaviour of existing membrane roof surfaces is necessary, and is the motivation behind this research.

When considering the development of a membrane roof, one of the fundamental issues that concerns engineers engaged in designing such structures is the displacement of the membrane surface under loading (Dakov and Tanev, 2005; Essrich, 2005). Lewis (2003) also highlighted a considerable need for further research into the interaction of surface geometry, applied loads and structural response. The overall aim of this project is therefore to obtain this information by developing a monitoring system capable of inspecting the dynamic behaviour of generic membrane roof structures. The geomatics technology of videogrammetry, which is capable of obtaining 3D models of dynamic objects, is introduced in the monitoring system. However, due to the constraints of the working environment, some traditional videogrammetric tasks were impractical and alternative techniques were therefore developed. Having proved to work satisfactorily under laboratory conditions, the prototype monitoring system was deployed to a real-world site in order to verify its feasibility.

This paper introduces firstly the methodology adopted by the monitoring system and then the software developed for processing the video image data and producing sequential surface models. The findings of the simulated experiments under laboratory conditions and, finally, the real-world fieldwork are analysed and presented.

Methodology

Background

Optical three-dimensional (3D) coordinate measurement via digital close range photogrammetry has often been applied for observing dynamic objects and tracking a moving trajectory (recent examples in a variety of applications include Fraser and Riedel, 2000; Harvey and Seager, 2001; Doucette et al., 2002; Maas et al., 2003; Nowacek et al., 2004; Holderied et al., 2005; Figueroa et al., 2006). This technique, which is also termed videogrammetry or vision metrology, offers a practical, inexpensive, non-interfering method of measurement (Ryall and Fraser, 2002). Black and Pappa (2003) further define videogrammetry as the science of calculating 3D object coordinates as a function of time from image sequences captured by video cameras. It expands the method of photogrammetry from still imagery to multiple time steps, enabling the observed object to be defined dynamically. This led to the adoption of

characteristic videogrammetry in the system for determining the dynamic behaviour of membrane roof surfaces.

When constructing a surface model by videogrammetry, it is common to use some form of targeting for control in order to determine the position and orientation of the cameras. Moreover, in order to determine a surface model, well-defined targets for image measurement should ideally be located extensively across the surface. Constraints, such as a uniform surface texture and unreachable height, involved in measuring membrane roof structures meant that traditional methods of targeting were generally not practicable. To solve these problems, alternative methods were adopted in this project.

Machine Vision CCD Cameras

Two machine vision CCD cameras, Oscar OF-810C models, were adopted as the sensors in the monitoring scheme, thanks to their advantages of compactness, light weight and good geometric stability (Maas and Hampel, 2006). The image features and image output were controlled and accomplished through the IEEE-1394 (Firewire) interface provided by the Oscar cameras. In order to acquire clear imagery of the dynamic membrane roof structures under test, the progressive scan shooting mode with imaging size of 1088 by 822 pixels was adopted for recording the image sequences in all the experiments discussed in this paper. To synchronise the two cameras during image capture, a pulse generator was introduced to transmit simultaneous signals to trigger the shutters of the cameras.

Immediately prior to monitoring, the two Oscar cameras, each fitted with a nominal 12 mm lens, were calibrated in a 3D close range calibration field. A total of 69 stick-on targets were arranged and four images at different rotation angles were taken from each of five camera stations. The calibration was carried out in the manner described by Mills et al. (2003), using a self-calibrating bundle adjustment in the VMS software.

Non-contact Control Method

A certain number of control points in object space are generally required for photogrammetric and videogrammetric applications. Object space coordinates of control points, which must be image-identifiable features, are normally determined in traditional close range photogrammetry via some type of field survey, usually employing a theodolite or total station. However, in this case it proved difficult to identify reliable features on the object or to attach physical targets to the surface that could act as control points. To accommodate this particular situation, a reflectorless electromagnetic distance measurement (EDM) technique offered an alternative solution whereby visible laser footprints were imaged by the video cameras being used to measure the scene. Because the footprints were visible in the acquired video images, and had associated 3D coordinates determined by the total station, they could be used as control points.

In the experiments a motorised total station (Leica TCRA1103, featuring a reflectorless EDM with a visible laser) was used to generate the laser footprint control. Once the total station was set up, a scan program was executed and a sequence of points measured directly on the surface of the membrane structure. Meanwhile the digital video cameras were arranged in the appropriate positions and triggered to acquire image sequences of the laser footprints. These laser footprints, complete with 3D coordinates, were recorded in different frames of the acquired image sequences (Fig. 1). The acquired images were combined using an image arithmetic algorithm to produce an image of all EDM laser footprints for each exposure station. The image coordinates of the laser footprints were then extracted automatically by a

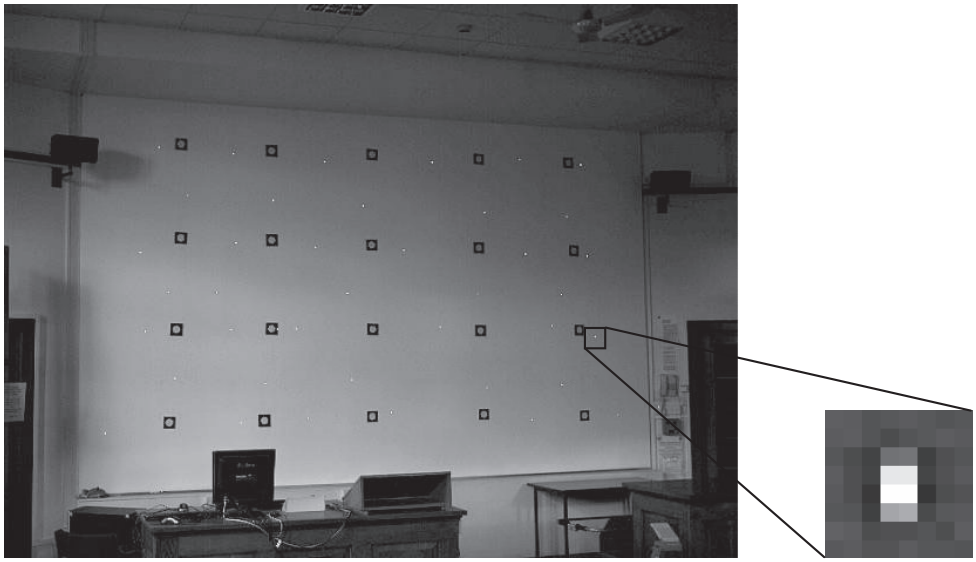

FIG. 1. EDM laser footprint, generated from a Leica TCRA1103 total station, and imaged using a digital video camera.

centroiding algorithm and introduced into the videogrammetric process as control points. Although the success of centroiding is heavily dependent on thresholding and image artefacts, making least squares matching methods a more favourable option, Maas and Kersten (1994) pointed out that no significant differences are found between the results of centroiding techniques and least squares matching. Moreover, Lin and Mills (2005) have shown the idea to be practicable and comparable to conventional control methods.

Videogrammetry using Projected Dots

A complete and accurate surface model will be determined from videogrammetry if there are sufficient artificial targets or natural features on the surface to be measured. However, as the membrane surfaces in question lacked identifiable texture and were unreachable, attaching targets was difficult, if not impossible. Moreover, as the membrane roof surface was thin and flexible, applying conventional targets on the surface would provide a loading and deform its original shape. Therefore, physically attached targets were substituted with a non-contact, structured light targeting method.

Structured light can be used either in an active or a passive manner (Maas, 1992b). For active structured light applications a light spot (or alternatively a line or grid) is generated by a laser and is recorded by a location-sensitive photoelectric detector. If the geometry of projection and recording device is known, the position of the light spot can be resolved (Fisher et al., 1999; Li and Zhang, 2004). On the other hand, passive structured light is used to supply a surface with an artificial texture by means of a projected random pattern. A 3D model of the surface in question can then be determined by correlating the pattern shown on the image recording devices (Maas, 1992a; D'Apuzzo, 2002; Schmidt and Tyson, 2003).

In other videogrammetric applications where the working requirements were similar to this monitoring scheme, the passive use of structured light has been adopted (Ganci and

Brown, 2000; Greenwood et al., 2001; Black and Pappa, 2003; Blandino et al., 2003; Pappa et al., 2003), whereby a regular pattern of dots is projected onto the surface of interest to replace physical targets. Due to the advantages of time-efficiency, greater flexibility for allowing customisation to any target density or size, relatively simple hardware and fast algorithms (Maas, 1992b), this method was introduced into the videogrammetric system for observing the dynamic movement. An appropriate pattern of regular circular dots was created as a slide in Microsoft PowerPoint software and continually projected onto the membrane surface using a data projector. The changes in position of the projected dots were then recorded over time by the video cameras.

It is noteworthy that dots which are projected, and which are therefore not physically attached to the membrane roof surface, cannot arbitrarily move in all directions when the surface vibrates or changes shape. The use of projected patterns thus allows no direct measurements of discrete object points. Instead, the path of each target as measured by videogrammetry always follows a straight line moving either towards or away from the projector, regardless of how the surface moves in reality (Maas, 1992b; Pappa et al., 2003). This limits the measurement system to out-of-plane (as opposed to in-plane) movements; however, in this monitoring scheme the dominant direction of displacement was expected to occur almost parallel to this direction, the method of using projected dots therefore providing satisfactory targeting.

Membrane Structure Monitoring System (MS^2) Software

For processing the acquired image data and determining the sequential surface model, an in-house software suite, the Membrane Structure Monitoring System (MS^2), was developed. Once the collection of the video imagery was completed, the measurement processes were subsequently implemented in MS^2 using the Camera Orientation, Target Extraction, Target Referencing, Target Tracking and Target Modelling modules. The computational sequence is indicated in Fig. 2.

SYSTEM PERFORMANCE

In order to assess the performance of the proposed monitoring system, two tests were conducted under laboratory conditions. Imagery was acquired of both a static and a dynamic surface and subsequently input into MS^2 for measurement. The tests were designed to simulate the type of network configuration that would be subsequently adopted in the field.

Static Surface Modelling

In the first test a static object (a laboratory internal wall) was selected and modelled using the developed videogrammetric system. The two Oscar cameras, each fitted with a nominal 12 mm lens, a Leica TCRA1103 motorised total station and a data projector (Philips ProScreen 4750) were arranged in a configuration simulating the test site for observing the wall surface. Fig. 3 indicates the two-station convergent network geometry, where the average camera-to-object distance for the two cameras was 10·0 m (image scale 1:900). With this stereo configuration of camera network, coupled with an image coordinate measurement precision via centroid targeting of 0·1 pixel, a measurement precision (at 68·3% probable error level) of close to ±1·4 mm could be anticipated for points across the surface (Karara and Abdel-Aziz, 1974). In addition, the video camera frame rates were set to 3 and 1 frames per second (fps) for

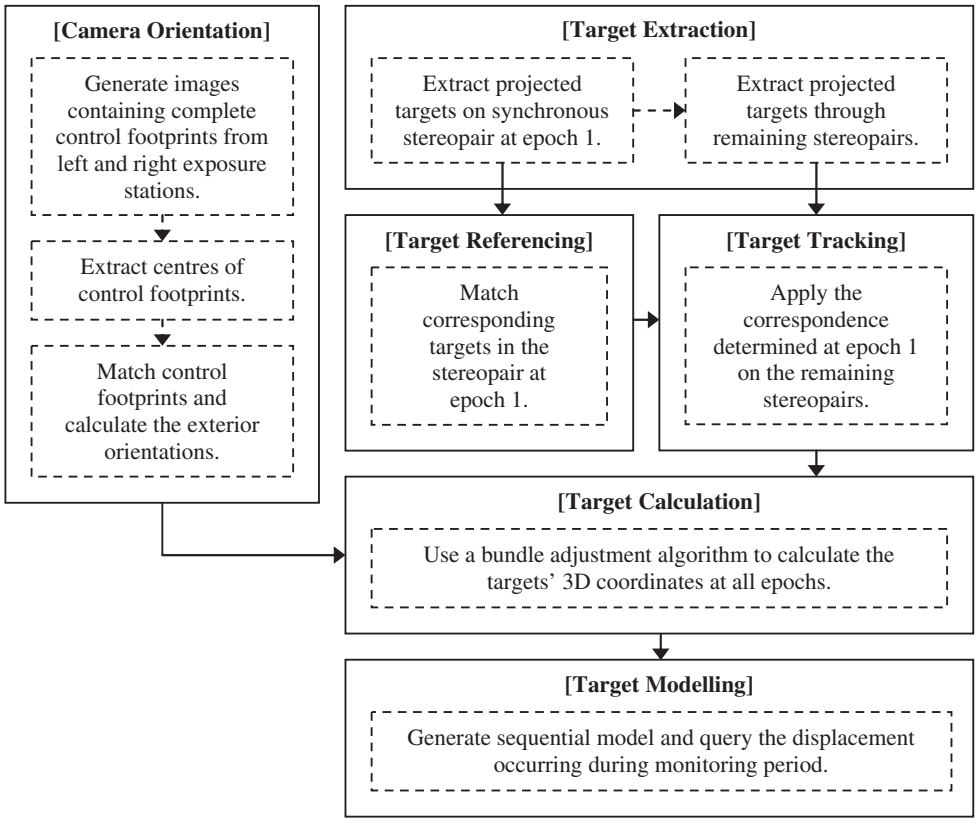

FIG. 2. Computational sequence of the measurement processes in MS^2.

collecting control laser footprints and projected dots, respectively. This setting would subsequently be applied on all the experiments described in this paper.

The previously described non-contact control method was adopted, generating 21 control footprints across the area being imaged. The image sequences were then processed in the Camera Orientation module in MS^2. Once complete, all the laser footprints were successfully extracted and the corresponding footprints were subsequently matched. The results were used for computing the exterior orientation parameters of the two cameras.

After the scanning of the control laser footprints, a dot pattern of 450 points was projected onto the wall and adopted as providing the targets for reconstructing the surface model. The frame rate of the cameras was adjusted to 1 fps and the monitoring continued for 500 s. For videogrammetric measurement the acquired stereopairs were processed in the Target Extraction module in MS^2 to derive the centres of all 450 points at each epoch. The resulting coordinates were saved and input to the remaining modules for further implementation of target referencing, tracking and calculation.

When the calculation in MS^2 was complete, the 3D position of each projected dot at each epoch was solved with a resultant standard deviation of 1·0 mm. The measurement precision was therefore shown to be of the same order as the value predicted in network pre-planning. In order to determine the displacement that occurred through the whole sequence, the surface

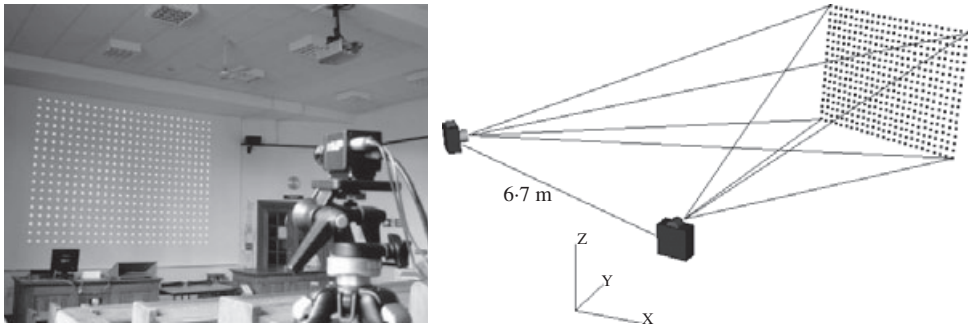

FIG. 3. Left: projected-dots pattern on the static wall, observed by the left camera. Right: videogrammetric network comprising two camera stations and the pattern of projected dots.

model from the first epoch was selected as the reference surface. The positive (points where forward movement occurred) and negative (backward) movements that occurred during the monitoring were computed separately.

Since the observed wall surface was static there should obviously be no movement determined by the measurement system. However, the mean and maximum displacements were solved as 0·8 and −0·8 mm, respectively. Comparison of these values against the measurement precision (±1·0 mm), suggests the resolved displacements are measurement noise rather than real movement. In addition to the non-zero mean movement, the resolved maximum displacements that occurred over 500 epochs varied from 6·2 to −5·8 mm. As the static surface modelling experiment was conducted in a well-controlled laboratory environment, the results were considered as the best performance the videogrammetric monitoring system could be expected to achieve. That is, when the system was subsequently applied in real-world dynamic monitoring tasks, the videogrammetric system was only able to detect displacements occurring above these threshold values. According to the design specification, the fabric membrane itself deflects significantly under extreme external loading, with predicted displacements in the middle of the panels occasionally in excess of ±250 mm (Bridgens et al., 2004). The monitoring system was therefore deemed capable of inspecting displacements within the tolerance value.

Dynamic Surface Modelling

In the dynamic surface modelling laboratory experiment, a projector screen was used to simulate the membrane roof surface to be observed at the real-world test site. The camera configuration previously described was once again set up, and the proposed equipment and methodology were applied to measure the surface movement, which was generated by manually shaking the screen.

Once the processing in MS^2 was complete, the camera orientation was determined using eight common control footprints (Fig. 4) and the 3D coordinates of 120 projected dots at each epoch were solved with a final precision of 1·3 mm. The value was again shown to be of the same magnitude as the predicted measurement precision at the network design stage. Fig. 5 illustrates an example session of the stereoscopic image sequence and the determined meshed model, showing the movement of the observed surface.

In order to determine displacement, the surface model at the first epoch was selected as the base surface, and the positive and negative movements that occurred during the monitoring

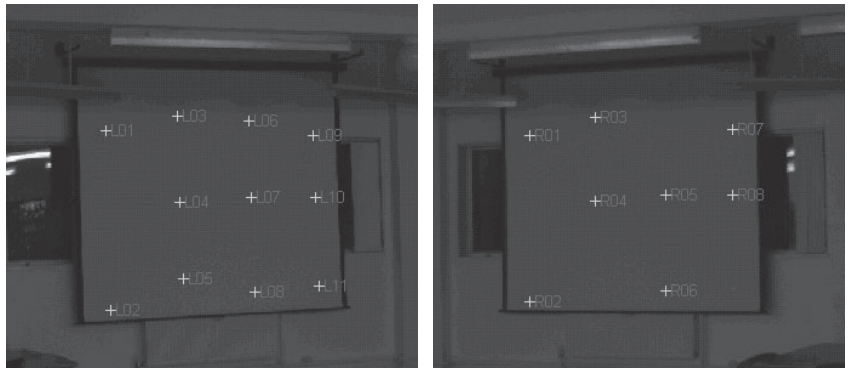

FIG. 4. Images of extracted control footprints from left and right exposure stations.

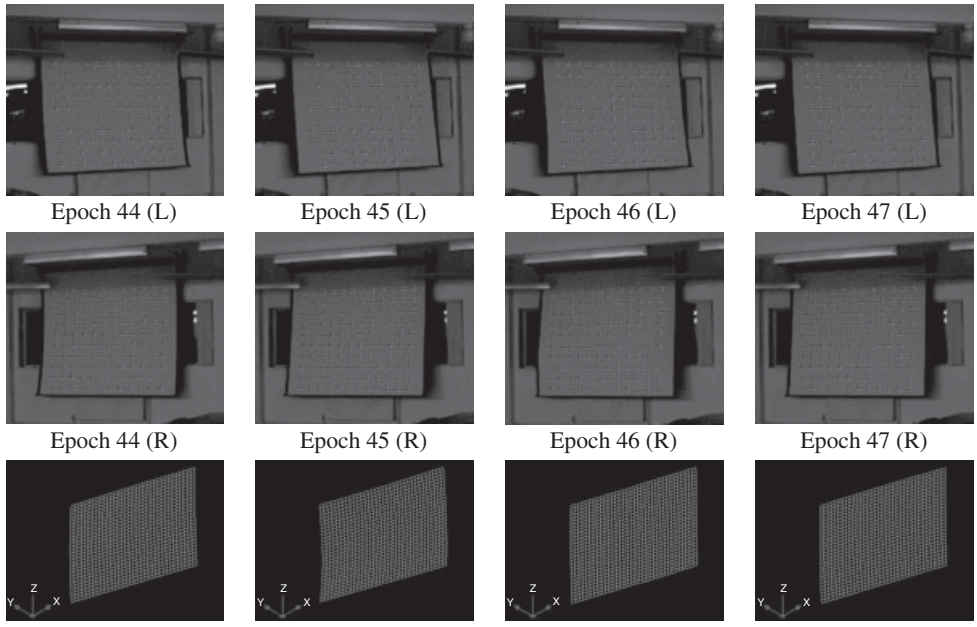

FIG. 5. Example image sequences of extracted projected targets from left and right exposure stations and the derived meshed model of the surface.

period were computed relative to this. The average and maximum displacements at each of the 180 epochs is illustrated in Fig. 6. In the initial period of monitoring the average positive and negative displacements varied from 0·9 to 1·1 mm (curves (b) and (d)), and the maximum movements were 5·6 and −6·3 mm (curves (a) and (e)) in positive and negative directions, respectively. This period related to the time when no movement was applied to the screen and can be seen to be generally commensurate with the findings derived from the static surface modelling test.

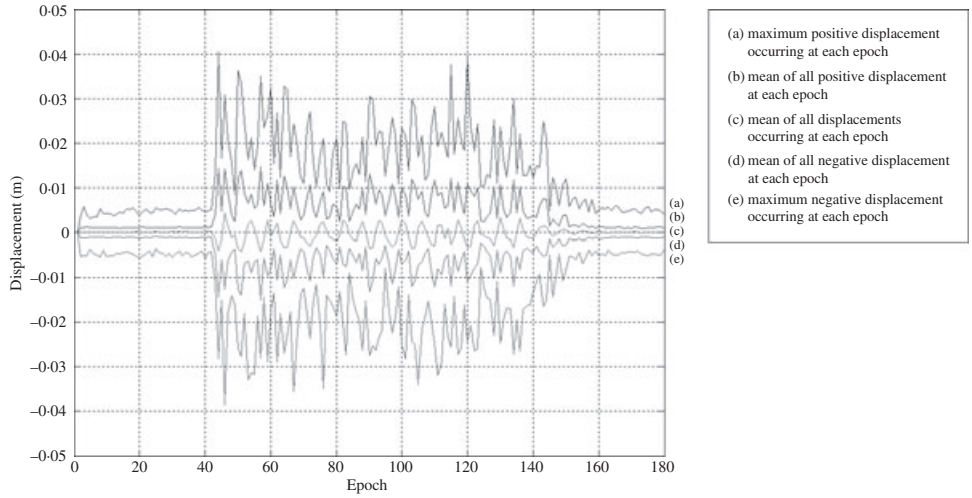

FIG. 6. Average and maximum movement that occurred at each epoch.

In comparison with the motionless period, it is clear from Fig. 6 that the movement started from around the 40th epoch and continued to the 150th epoch. Fig. 6 shows that the maximum positive movement of 40·4 mm occurred at the 44th epoch, whilst the maximum negative displacement of −38·6 mm occurred at the 46th epoch. According to the curve of displacement it is shown that the surface remained stationary again after the 160th epoch until the end of monitoring.

ON-SITE IMPLEMENTATION

Having proved to work well under laboratory conditions, the developed system was deployed to a real-world site (Dalton Park, a retail outlet centre in the north-east of England). The membrane structures at Dalton Park are categorised as conical-shaped boundary-tensioned membranes. Two different types and dimensions of "Tents" were selected to verify the feasibility and transferability of the videogrammetric monitoring system.

In addition to the videogrammetric monitoring, the technique of terrestrial laser scanning was introduced in the fieldwork to provide as-built records of the membrane structures. Both Leica HDS2500 and HDS3000 laser scanning systems were adopted to create the as-built models of each membrane structure. As the videogrammetric and the laser-scanned models were constructed under the same coordinate system, the two models could be combined. This enabled visualisation of the area of the membrane roof where the targets were projected.

Tent Type 1

Tent Type 1 is illustrated in Fig. 7. It consists of a fabric membrane of conical shape; the size of the membrane roof is approximately 14·4 m × 14 m, with the top circular ring being 12 m above ground level.

The two Oscar cameras, equipped with the nominal 12 mm lenses and image size of 1088 × 822 pixels, were used for videogrammetric data acquisition. Under given workplace constraints they were arranged in an appropriate network for covering the area of projection, at

FIG. 7. Observed membrane structure (Type 1) and its laser-scanned model.

which the average camera-to-object distance was 9·4 m and the image scale was approximately 1:800. Fig. 8 illustrates the two-camera configuration and the area of target projection. Once the total station and the data projector were set up, the cameras were triggered by the signals transmitted from the pulse generator to collect image sequences of the control laser footprints and the projected-dot targets. Afterwards the acquired imagery was input to MS^2 for videogrammetric measurement, from which the images of complete control laser footprints and projected dots were derived, as shown in Fig. 9. The projected target coordinates were solved and the resulting precisions, derived from a bundle adjustment, were 0·5, 0·6 and 1·1 mm in X, Y and Z axes, respectively.

Stereopairs of 500 epochs were collected and a total of 638 points were recorded at each epoch. The surface derived at the first epoch was selected as the base model and the displacements that occurred over the subsequent 499 epochs were determined and are shown in Fig. 10. Although some evidence of movement could be observed, analysis showed the figures to be similar to those derived from the static surface modelling test, with the maximum positive and negative displacements of 6·3 and −6·2 mm being of the same order of magnitude as the minimum movement that could be inspected using the system. This indicated that there was no

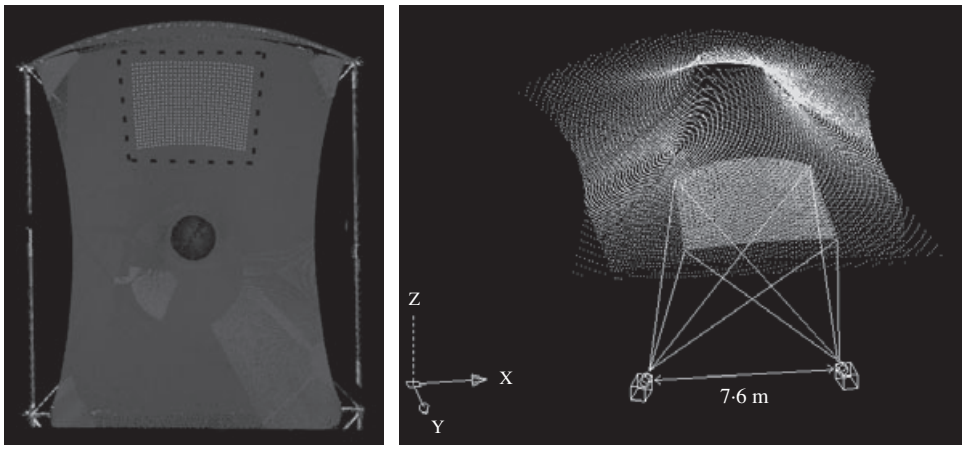

FIG. 8. Laser-scanned model and videogrammetric monitoring area (outlined by dashed line) on Tent Type 1.

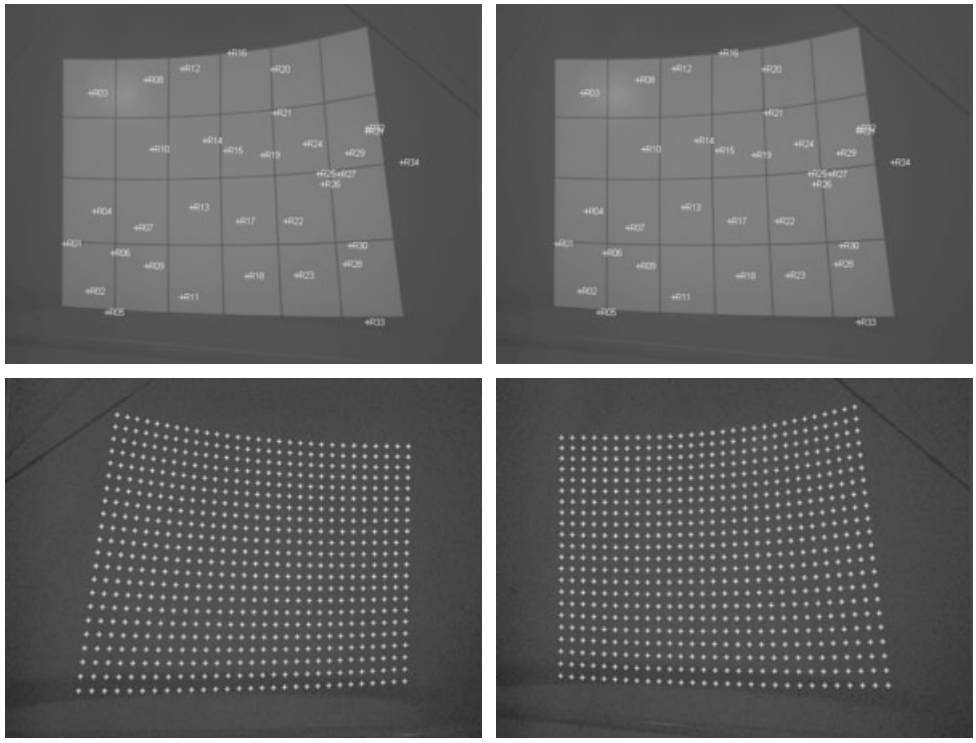

FIG. 9. Stereopair of extracted control footprints and projected dots.

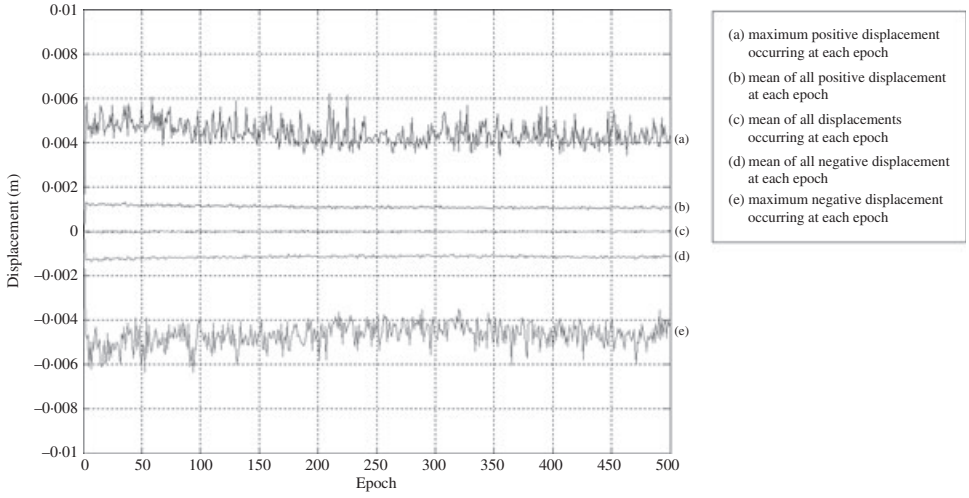

FIG. 10. Resulting displacements for the observations on the Type 1 membrane structure.

unexpected movement being observed by the videogrammetric monitoring system. As the weather conditions were good on the day the experiment was conducted this result, in which the observed displacements in the sequential surface model were largely insignificant, was as expected for a membrane structure in serviceable condition.

Tent Type 2

The Type 2 membrane structure was similar to the Type 1 with the exception of the flying mast design (Fig. 11). In the Type 1 membrane structure the flying mast was propped up vertically while it was tilted in the Type 2 structure. The dimensions of the structure were 12 m × 18 m in plan, with the highest point being approximately 12 m above ground level. Based on the same workflow mentioned in the previous experiments, the videogrammetric system was arranged to collect the image sequences (Fig. 12). The average camera-to-object distance was 11·2 m and the predicted precision was 1·5 mm. In this fieldwork the observation duration was extended to 1 h in order to cover more complete movements. The positions of the control laser footprints and projected dots were derived (Fig. 13). The 3D coordinates of each projected target over 3600 epochs were solved with the measurement precision of ±1·6 mm.

Over 3600 epochs were analysed to determine the displacements of the Type 2 membrane structure. Fig. 14 shows that numerous dramatic movements were observed over the period of monitoring. From the derived statistics the maximum positive displacement was 22·9 mm (at

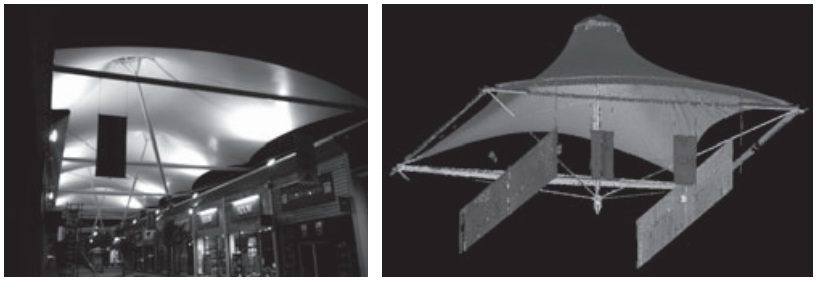

FIG. 11. Observed membrane structure (Tent Type 2) and its laser-scanned model.

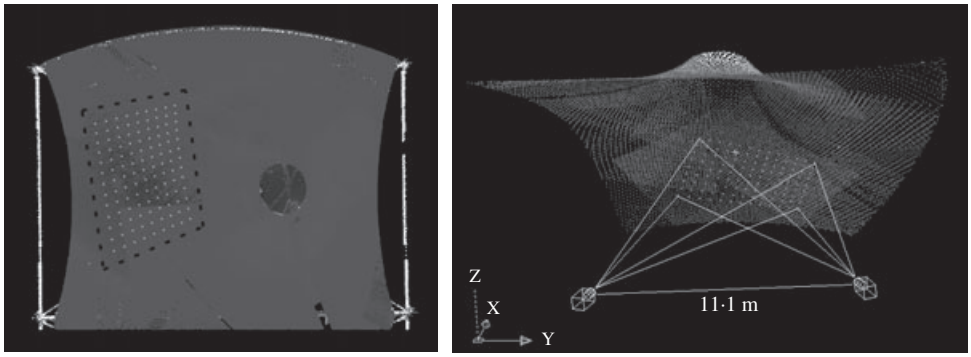

FIG. 12. Laser-scanned model and videogrammetric monitoring area (outlined by dashed line) on Tent Type 2.

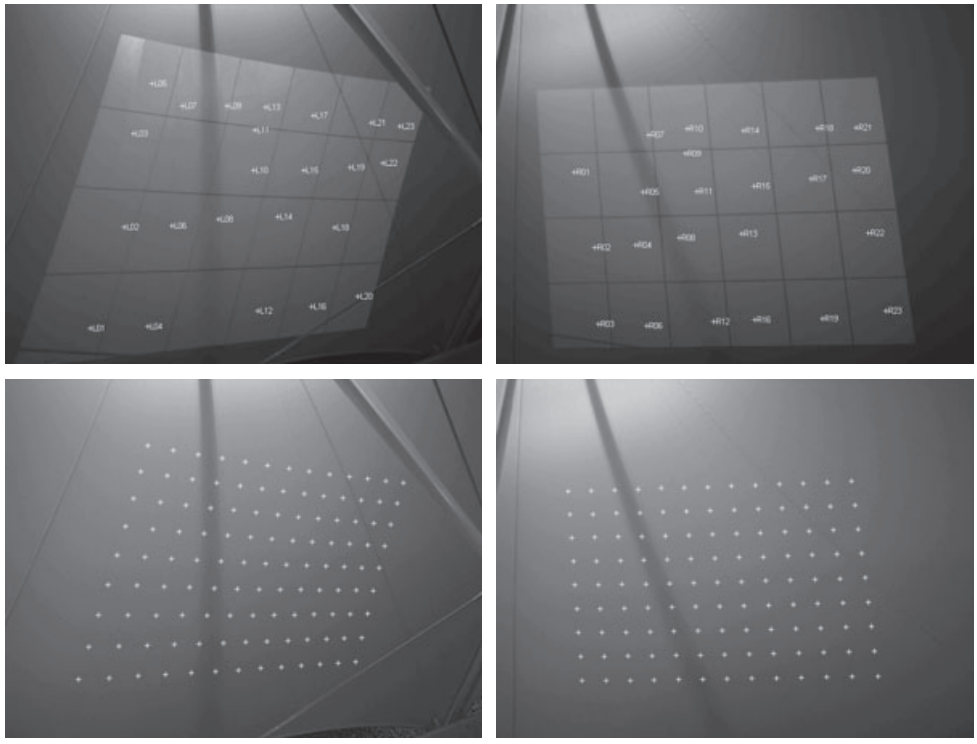

FIG. 13. Stereopairs of extracted control footprints and projected dots.

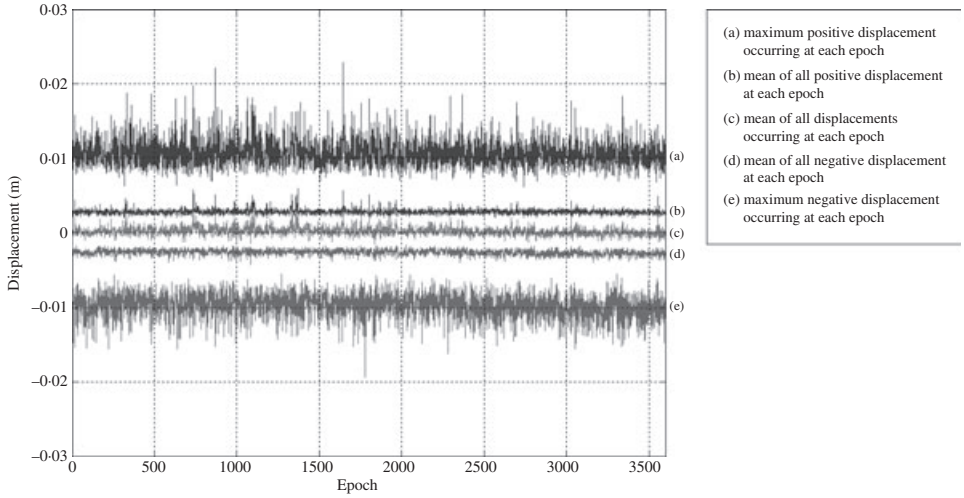

FIG. 14. Resulting displacement for the observations on the Type 2 membrane structure.

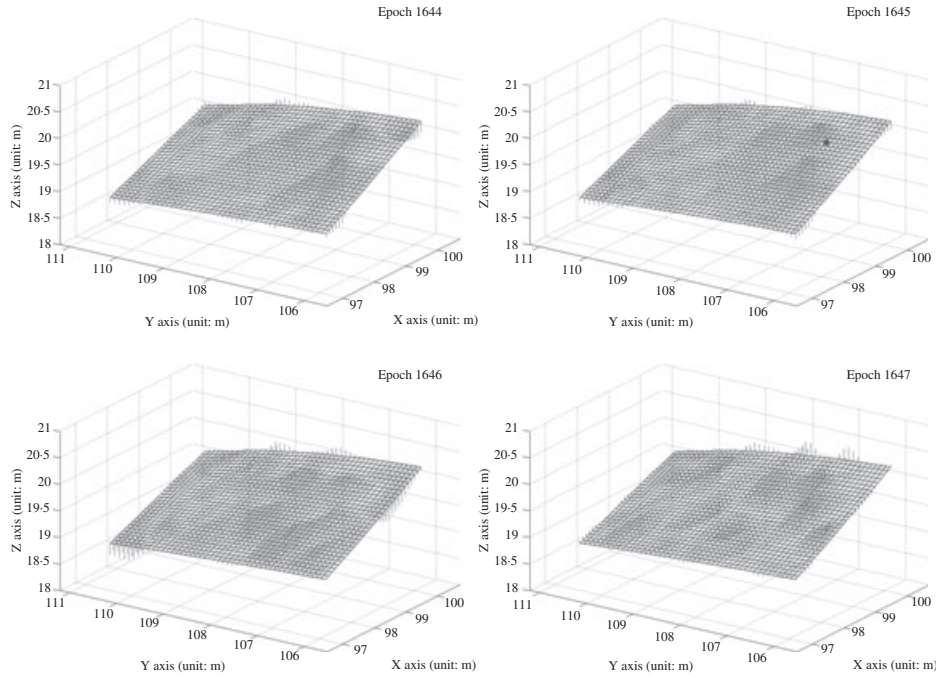

FIG. 15. The displacement map of the observed surface. The base is the surface model of the first epoch, the vectors (which are 3 times magnified) represent the differences to the specific epoch.

epoch 1645), while the maximum negative movement was −19·4 mm (at epoch 1777). The movements were suspected to be caused primarily by external wind loading.

As the maximum positive displacement occurred at the 1645th epoch, the sequential model around it was further analysed in order better to understand the dynamic behaviour of the surface. Firstly a displacement map was generated, in which vectors were plotted to represent the differences of *Z*-ordinates between the base surface and any model of specific epoch. The displacement maps of epochs 1644 to 1647 are shown in Fig. 15, allowing the areas of apparent movements to be analysed; for example, the location of the maximum positive displacement of the 1645th epoch was determined at (99·4 m, 107·1 m), as highlighted by a blue point in Fig. 15.

In addition to the 3D displacement map, 2D profiles across the membrane surface were also extracted. Two profiles passing through the point (99·4 m, 107·1 m) in the sequential meshed model are depicted in Fig. 16, the differences in profiles between the base and the specific surface models are also illustrated. Along the profiles where $X = 99{\cdot}4$ m it is shown that obvious movements occurred between $Y = 106{\cdot}0$ and $108{\cdot}0$ m. Along the profile $Y = 107{\cdot}1$ m, large displacements are apparent in two sections where $X = 97{\cdot}5$ to $98{\cdot}5$ m and $X = 99{\cdot}0$ to $100{\cdot}0$ m.

DISCUSSION

Non-contact Targeting Methods

During the videogrammetric monitoring described, non-contact targeting methods were adopted to produce the laser footprints for control and also the projected dots for surface

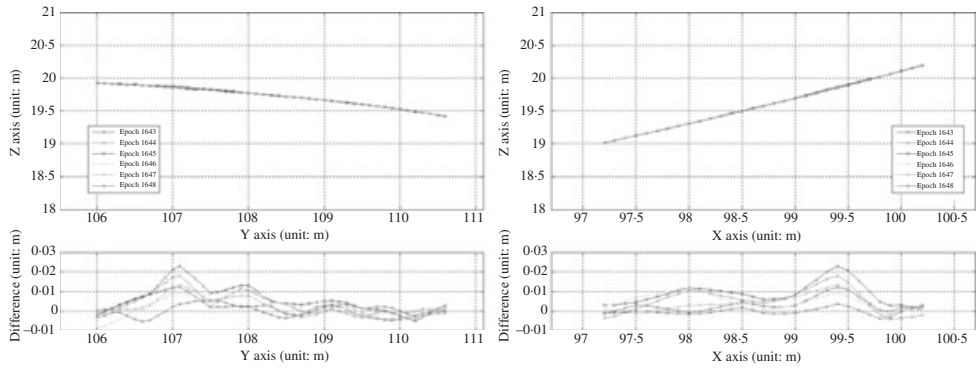

FIG. 16. Two profiles across the observed membrane roof (left: profile along Y axis where $X = 99{\cdot}4$ m; right: profile along X axis where $Y = 107{\cdot}1$ m).

modelling. Although the implementation of automated target extraction was fully supported in MS^2, some discussion is considered necessary. Firstly, due to the small size of the control footprints produced by the EDM, it was sometimes difficult to distinguish control footprints from image noise. Secondly, in some experiments it was noted that some control laser footprints were missed in the final control footprint imagery. This was affected by the threshold value used for image segmentation in the target extraction stage. This resulted primarily from some laser footprints of low colour contrast being ignored after image segmentation. Additionally, as two different threshold values were applied on the images taken from left and right exposure stations, the missing footprints may be varied between the stereopairs. An increased image sequence frame rate may solve the problem; however, the storage space for recorded imagery would need to be augmented. As the number of missing control footprints insufficiently affected the performance of camera orientation (as long as more than 10 laser footprints were available, as explained later), a frame rate of 3 fps during capture of the laser control footprints produced acceptable results.

The final consideration relates to the execution of projected-dot videogrammetry. The shooting of projected dots took place at night in order to make use of a relatively low-powered data projector, although this limitation could potentially be overcome by using a projector with a brighter lamp.

Consistency of On-site Non-contact Control

In addition to the standard monitoring task, the consistency of non-contact control implementation on-site was inspected. The operation of generating and recording laser footprints was conducted 3 times at the beginning and repeated twice at the end of the Type 2 monitoring campaign. The data derived from each set was input to MS^2 for footprint extraction and matching. As a result, a total of 20, 22, 23, 21 and 23 common points were obtained respectively from the five scanning tasks. Consequently, six footprints located evenly across the observed area were specified as check points in each task and diverse numbers of remaining footprints were systematically selected as control points, to estimate the rms error values of the remaining check points. A plot of accuracy against the number of control points employed is depicted in Fig. 17. In general, higher accuracy is achieved by adopting more control points in the computation, however, rms errors are shown to become more stable when at least 10 control points are employed. When 10 control points

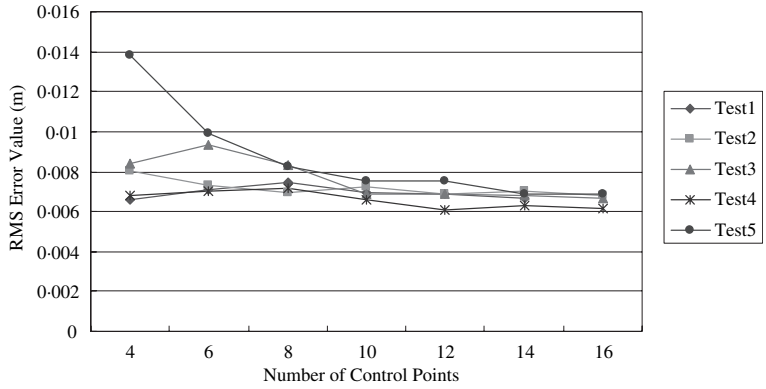

FIG. 17. A graph of the rms error values versus diverse numbers of adopted control points.

were used the rms errors ranged from 6·7 to 7·5 mm. The accuracies of the same order demonstrate the consistency of the on-site non-contact control approach, although on-site results were slightly degraded compared with those obtained in the indoor experiments. Moreover, as the monitoring was performed outdoors, the exterior orientation of cameras might change due to changing environmental conditions such as temperature and wind during a monitoring survey. Whilst the accuracy checking implemented here demonstrates the stability of the overall monitoring system, further refinements should be made to monitor the stability of the system during monitoring (for example, by monitoring fixed points in the scene, if possible).

Videogrammetric Measurement Performance

To achieve advanced measurement performance in photogrammetric applications of static object modelling, one camera is normally used to capture images of the object in different, redundant, positions and angles. However, in most dynamic surface monitoring tasks, as the images need to be taken simultaneously, the cameras have to be arranged in fixed positions during the monitoring period. Therefore, the number of cameras adopted becomes a factor mainly affecting the measurement precision. In the videogrammetric monitoring system described, two machine vision CCD cameras were used. Based on the camera network employed and image mensuration precision, the precisions derived from the Type 1 and Type 2 membrane monitoring schemes were respectively 1·3 and 1·6 mm in object space. Such results are adequate for the membrane roof structure monitoring task, but could be improved by deploying more cameras in a stronger network configuration. For example, the precision could be expected to improve to between 0·6 and 0·8 mm if one more camera was adopted (Fraser, 2001). However, accompanying issues of image storage space and processing efficiency, but primarily of cost, would also need to be considered. The final solution would be a compromise between required precision, processing time and budget limitations.

Displacement of Membrane Roof Structures

Obvious movements caused by external wind loading occurred over the Type 2 membrane roof structure observed in the monitoring campaign. Within various load types, Essrich (2005) emphasised that wind loads are very significant in the case of membrane buildings, however,

the current methods of structural calculation for correcting the membrane shape were either too expensive (wind tunnel tests) or not rigid enough (experiences from wind specialists). Therefore, the videogrammetric monitoring system proposed in this paper offers an ideal solution for determining the as-built movement under external loading. The measured displacement data was therefore delivered to structural engineers for proprietary analysis.

From the perspective of building construction, once the arrangement of supports for a membrane structure has been established, any change of position, length or angle of compression member results in an immediate change of volume, form and structural behaviour (Scheuermann and Boxer, 1996). Therefore, the movements may result from either improper design in the planning stage or incorrect erection during construction. For further investigation of the factors causing the displacements, a comparison could be made between the original designed mathematical model and the as-built finished model of the membrane structure produced by using terrestrial laser scanning methods (see Lin and Mills, 2006).

CONCLUSION

A monitoring system that applies videogrammetry has been developed to realise the dynamic behaviour of membrane roof structures. In the videogrammetric monitoring task, a non-contact targeting method was used in order to accommodate the constraints of the working environment. By analysing a sequence of surface models, displacement and deformation of two types of membrane roof structure were successfully determined over time. The information acquired by the system is proving to be of great value to collaborating engineers who are involved in the design and refinement of such membrane structures.

ACKNOWLEDGEMENTS

The authors would like to thank Arup for providing the mathematical model of the Dalton Park membrane structure. The authors also thank the staff at Dalton Park for their help in making the fieldwork run smoothly.

REFERENCES

BLACK, J. T. and PAPPA, R. S., 2003. Videogrammetry using projected circular targets: proof of concept test. http://techreports.larc.nasa.gov/ltrs/PDF/2003/tm/NASA-2003-tm212148.pdf [Accessed: 2nd February 2008].

BLANDINO, J. R., PAPPA, R. S. and BLACK, J. T., 2003. Modal identification of membrane structures with videogrammetry and laser vibrometry. American Institute of Aeronautics and Astronautics Paper 2003–1745: 11 pages.

BRIDGENS, B. N., GOSLING, P. D. and BIRCHALL, M. J. S., 2004. Tensile fabric structures: concepts, practice & developments. *Structural Engineer*, 82(14): 21–27.

DAKOV, D. and TANEV, V., 2005. Experimental investigation of a conical shaped textile membrane under snow loading. *TensiNews*, 8: 12–13.

D'APUZZO, N., 2002. Surface measurement and tracking of human body parts from multi-image video sequences. *ISPRS Journal of Photogrammetry & Remote Sensing*, 56(5): 360–375.

DOUCETTE, J. S., HARVEY, E. S. and SHORTIS, M. R., 2002. Stereo-video observation of nearshore bedforms on a low energy beach. *Marine Geology*, 189(3): 289–305.

ESSRICH, R., 2005. *From Draft Design to Installation*. Lecture handout from Textile Roofs 2005 Workshop, Berlin. 14 pages.

FIGUEROA, P. J., LEITE, N. J. and BARROS, R. M. L., 2006. Tracking soccer players aiming their kinematical motion analysis. *Computer Vision and Image Understanding*, 101(2): 122–135.

FISHER, R. B., ASHBROOK, A. P., ROBERTSON, C. and WERGHI, N., 1999. A low-cost range finder using a visually located structured lightsource. *Proceedings of 2nd International Conference on 3-D Digital Imaging and Modeling*, Ottawa, Canada: 24–33.

FRASER, C. S., 2001. Network design. *Close Range Photogrammetry and Machine Vision* (Ed. K. B. Atkinson). Whittles, Caithness. 371 pages: 256–281.

FRASER, C. S. and RIEDEL, B., 2000. Monitoring the thermal deformation of steel beams via vision metrology. *ISPRS Journal of Photogrammetry & Remote Sensing*, 55(4): 268–276.

GANCI, G. and BROWN, J., 2000. Developments in non-contact measurement using videogrammetry. http://www.geodetic.com/Downloadfiles/Developments%20in%20Non%20Contact%20Videogrammetry.pdf [Accessed: 2nd February 2008].

GOSLING, P. D., 2001. Non-linear material models for coated woven fabrics. http://www.staff.ncl.ac.uk/p.d.gosling/pdg/arup.pdf [Accessed: 23rd January 2007].

GREENWOOD, J. A., DARVE, C., BERNSTEIN, R., BLACK, E. and KUBIK, D., 2001. Failure-mode metrology using projected target videogrammetry. http://tdserver1.fnal.gov/nicol/lhc_irq_cryostat/ch_darve/public/publi/photogrammetry.pdf [Accessed: 2nd February 2008].

HAPPOLD, E., EALEY, T. A., LIDDELL, W. I., PUGH, J. W. E. and WEBSTER, R. H., 1987. The design and construction of the Diplomatic Club, Riyadh. *Structural Engineer*, 65A(1): 15–26.

HARVEY, E. S. and SEAGER, J., 2001. The validation of the accuracy and precision of *in situ* length measurements of Southern Blue Fin Tuna by stereo-video. http://www.afma.gov.au/research/reports/2000/r00_1181.pdf [Accessed: 2nd February 2008].

HOLDERIED, M. W., KORINE, C., FENTON, M. B., PARSONS, S., ROBSON, S. and JONES, G., 2005. Echolocation call intensity in the aerial hawking bat *Eptesicus bottae* (Vespertilionidae) studied using stereo videogrammetry. *Journal of Experimental Biology*, 208(7): 1321–1327.

KARARA, H. M. and ABDEL-AZIZ, Y. I., 1974. Accuracy aspects of non-metric imageries. *Photogrammetric Engineering*, 40(9): 1107–1117.

LEWIS, W. J., 2003. *Tension Structures: Form and Behaviour*. Thomas Telford, London. 201 pages.

LI, Y. F. and ZHANG, B., 2004. A method for 3D measurement and reconstruction for active vision. *Measurement Science and Technology*, 15(11): 2224–2232.

LIN, S.-Y. and MILLS, J. P., 2005. A non-contact method of controlling videogrammetry in surface modelling applications. *Optical 3-D Measurement Techniques VII* (Eds. A. Gruen and H. Kahmen). Vienna, Austria. Volume II: 124–132.

LIN, S.-Y. and MILLS, J. P., 2006. A non-contact monitoring system for investigating as-built membrane roof structures. *International Archives of Photogrammetry, Remote Sensing and Spatial Information Sciences*, 36(5): 161–166.

MAAS, H.-G., 1992a. Complexity analysis for determination of image correspondences of dense spatial target fields. *International Archives of Photogrammetry and Remote Sensing*, 29(B5): 102–107.

MAAS, H.-G., 1992b. Robust automatic surface reconstruction with structured light. *International Archives of Photogrammetry and Remote Sensing*, 29(B5): 709–713.

MAAS, H.-G. and KERSTEN, T. P., 1994. Experiences with a high resolution still video camera in digital photogrammetric applications on a shipyard. *International Archives of Photogrammetry and Remote Sensing*, 30(5): 250–255.

MAAS, H.-G., HENTSCHEL, B. and SCHREIBER, F., 2003. An optical triangulation method for height measurements on water surfaces. *Videometrics VIII*. SPIE 5013: 103–109.

MAAS, H.-G. and HAMPEL, U., 2006. Photogrammetric techniques in civil engineering material testing and structure monitoring. *Photogrammetric Engineering & Remote Sensing*, 72(1): 39–46.

MILLS, J. P., SCHNEIDER, D., BARBER, D. M. and BRYAN, P. G., 2003. Geometric assessment of the Kodak DCS Pro back. *Photogrammetric Record*, 18(103): 193–208.

NOWACEK, S. M., WELLS, R. S., OWEN, E. C. G., SPEAKMAN, T. R., FLAMM, R. O. and NOWACEK, D. P., 2004. Florida manatees, *Trichechus manatus latirostris*, respond to approaching vessels. *Biological Conservation*, 119(4): 517–523.

PAPPA, R. S., BLACK, J. T., BLANDINO, J. R., JONES, T. W., DANEHY, P. M. and DORRINGTON, A. A., 2003. Dot-projection photogrammetry and videogrammetry of gossamer space structures. http://techreports.larc.nasa.gov/ltrs/PDF/2003/tm/NASA-2003-tm212146.pdf [Accessed: 2nd February 2008].

PARKER, D., 1999a. Dome supplier faces Montreal compensation battle. *New Civil Engineer*, 28 January: 4.

PARKER, D., 1999b. Are giant tents domed? *New Civil Engineer*, 4 February: 16–19.

RYALL, T. G. and FRASER, C. S., 2002. Determination of structural modes of vibration using digital photogrammetry. *AIAA Journal of Aircraft*, 39(1): 114–119.

SCHEUERMANN, R. and BOXER, K., 1996. *Tensile Architecture in the Urban Context*. Butterworth Architecture, Oxford. 217 pages.

SCHMIDT, T. and TYSON, J., 2003. Full-field dynamic displacement and strain measurement using advanced 3D image correlation photogrammetry. *Experimental Techniques*, 27(3): 41–44.

Résumé

On a mis en œuvre un système de suivi basé sur l'emploi des techniques géomatiques, notamment à l'aide d'un balayage par un laser au sol et de vidéo-photogrammétrie, afin d'examiner le comportement dynamique des structures d'un toit réalisé à partir de membranes. Pour résoudre les problèmes rencontrés dans les mesures sur de telles structures, dus par exemple à l'uniformité de la texture des membranes et à l'inaccessibilité de leur hauteur, on a adopté une méthode de balisage sans-contact, à la place des techniques classiques de détermination des points d'appui. On a développé un logiciel spécifique pour traiter l'imagerie vidéo obtenue et établir un modèle numérique séquentiel de la surface de la membrane. On décrit d'abord dans cet article les essais de validation menés avec ce système de suivi pour s'assurer qu'il pouvait déterminer les surfaces testées avec une précision meilleure que ±1 mm. On a ensuite montré la faisabilité et la portabilité du système en établissant un polygone d'essais sur lequel on a mené des campagnes de suivi vidéogrammétrique avec données réelles et étudié deux types différents de structures à membranes. Les modèles séquentiels 3D de surface résultants ont permis d'étudier les déformations de la surface des membranes pendant toute une période au cours de laquelle les mouvements des membranes ont dépassé 20 mm. Les résultats ainsi obtenus se sont révélés d'un grand intérêt pour les ingénieurs impliqués dans la recherche et le développement sur ces structures à membranes.

Zusammenfassung

Es wurde ein Überwachungssystem mit geomatischen Komponenten inklusive Videogrammetrie und terrestrischem Laserscanning entwickelt, um das dynamische Verhalten von "as-built" Membrandachstrukturen zu ermitteln. Das System stützt sich auf berührungslose Techniken, um klassische Kontrollmessungen auch bei gleichförmiger Oberflächentextur und unerreichbarer Höhe zu ersetzen. Es wurde eine eigene Software für die Bearbeitung der erfassten Videobilder zur Erstellung eines sequentiellen Oberflächenmodells der Membran entwickelt. Dieser Beitrag berichtet zunächst über Untersuchungen, die zeigen, dass das Überwachungssystem in der Lage ist, repräsentative Teststrukturen mit einer Präzision von besser als ±1 mm zu erfassen. Danach wurden Messkampagnen an zwei verschiedenen Membranstrukturen mit dem Überwachungssystem durchgeführt, um die Anwendbarkeit und die Übertragbarkeit des Systems nachzuweisen. Die erzeugten sequentiellen 3D Oberflächenmodelle erlaubten die Untersuchung der Versetzung der Membranoberflächen, wobei der Umfang der Bewegung über 20 mm betrug. Die Information die dieses System liefert ist wertvoll für Ingenieure, die in Forschung und Entwicklung solcher Membranstrukturen beschäftigt sind.

Resumen

Se ha desarrollado un sistema de monitorización que usa técnicas geomáticas tales como la videogrametría y el escaneado láser terrestre, para investigar el comportamiento dinámico de estructuras de cubierta laminar una vez construidas. Para solventar los problemas de medida de estas cubiertas tales como lo puedan ser las texturas uniformes de la superficie y su altura que las hace inalcanzables, el sistema adopta una metodología de señalizado sin contacto para sustituir a las

técnicas de control tradicionales. Se elaboró un programa propio para procesar las imágenes de vídeo obtenidas y calcular un modelo de superficies secuencial de la membrana. Este artículo describe primero los experimentos llevados a cabo para demostrar que el sistema de monitorización era capaz de medir estructuras de prueba representativas con una precisión mayor de ±1 mm. Para demostrar la viabilidad y aplicabilidad del sistema, se realizaron campañas de monitorización videogramétrica en un área de ensayo real con dos tipos de cubiertas laminares. Los modelos de superficie tridimensionales secuenciales calculados permitieron investigar el desplazamiento de la superficie de la membrana a lo largo de un cierto período, durante el cual el movimiento observado alcanzó los 20 mm. La información obtenida con el sistema ha demostrado tener una gran importancia para los ingenieros de estructuras que trabajan en la investigación y la utilización de estas estructuras laminares.

